Diesel Generator Modelling for Microgrid Power Plant Parameters Assessment

CCTC 2015 Paper Number 1570034243

T. A. Theubou Tameghe[1], R. Wamkeue[2] and I. Kamwa[3]
[1]Université du Québec à Chicoutimi (UQAC), Québec, Canada
[2]Université du Québec en Abitibi-Témiscamingue (UQAT), Québec, Canada
[3]Institut de recherche d'Hydro-Québec (IREQ), Québec, Canada

Abstract

Successful control, identification, stability and diagnosis analysis of diesel generator set (DGS) based hybrid power plants depend on the efficient and reliable modelling of their main components. Unfortunately, there are several key parameters used to characterize the DGS which are not usually available. Accordingly, this paper presents a closed-loop model and parameters identification procedure of a commercial DGS unit. Dynamic behavior of the diesel prime mover with its governor, synchronous generator, excitation system (including the automatic voltage regulator (AVR)) is addressed. The effectiveness of the proposed DGS estimation approach is demonstrated through comparisons between model predictions and experimental data obtained from a 6.5-kVA 5-kW, 60-Hz laboratory DGS driven by a 7.2-hp diesel engine.

Keywords: Diesel generator set, synchronous generator, speed governor, automatic voltage regulator, identification, experimental validation.

Résumé

L'identification, l'analyse de stabilité, et la commande d'un système de cogénération faisant intervenir des générateurs diesel, passe par la modélisation de ses principales composantes. Cependant, plusieurs paramètres nécessaires à la caractérisation d'un groupe diesel ne sont en général pas disponibles. Pour combler ce manque, le présent article propose une nouvelle approche permettant d'estimer les paramètres en boucle fermée d'un groupe diesel usuel. Les modèles dynamiques de la turbine diesel, de la génératrice synchrone ainsi que les différents régulateurs (vitesse et tension) sont présentés. L'efficacité de la procédure d'identification et des modèles proposés est démontrée par des comparaisons entre les simulations et les données expérimentales obtenues d'un groupe diesel de laboratoire de 6,5-kVA/5-kW/60-Hz entrainé par un moteur diesel de 7,2-ch.

Mots clés : groupe diesel, génératrice synchrone, régulateur de vitesse, régulateur de tension, identification, validation expérimentale

1. Introduction

According to the green energy production emerging policies, cogeneration power plant schemes integrating renewable and conventional electrical power sources stand as the most viable solutions [1]-[3]. They are especially recommended for supplying isolated areas. Such regions are usually fed by diesel or micro-hydro power sources requiring continuous operation and high storage capacity of the primary source [3]. Given their low cost, reduced maintenance and robustness, diesel generators sets (DGSs) are the most commonly used conventional sources.

In order to reduce the fuel consumption and gas emissions of the diesel engines, wind turbines (WT) and solar panels are increasingly added to existing isolated power plants. When feeding an isolated load or an autonomous microgrid, the DGS source is well-known as stable and robust. However, instability may appear when they are connected in cogeneration scheme with mostly fluctuating energy sources such as WT or solar panels [3]-[6]. In addition, the risk of instability increases with the penetration level of renewable sources. A good prediction model of the classical DGS can efficiently assist in improving the reliability of a microgrid power plant, in particular, when operating in islanded mode [3]. In [5] and [6], effects of wind power penetration and regulation schemes for wind-diesel power plants as well as their performance prediction using PID controllers are proposed. Authors demonstrated the great impact of wind penetration on the system's time-domain transient responses.

The complexity of the diesel system leads to the use of lumped models. This is also the current practice in many other papers where basic empirical input-output relationships are written to predict DGS transients [7]-[8]. Besides this, intensive literature presents more or less accurate models (depending on the intended usage) of different constituents of a DGS [9]-[14]. However, there is a gap to be filled with regard to the identification of the DGS with its main control loop (frequency and voltage regulators).

This work is mainly motivated by the fact that in practice, a diesel generator is a very compact structure. In such a context, splitting it into its components to apply classical identification procedures is usually not an option [13]-[15]. The paper is organized as follows: in section II, the block diagram of a typical DGS is presented with emphasis on its two main parts (mechanical and electrical). An overview of the parameters identification process is also addressed. The state modelling of the DGS components is carried out in section III along with the design of identification tests. The estimation process is proposed in section IV. Finally, section V deals with obtained results and discussions.

2. Diesel genset overview and identification problem statement

2.1 Diesel genset overview

The block diagram of DGS is shown in Figure 1 [4], [6]-[9]. It consists of two parts: (a) the diesel engine, (b) the driven synchronous generator (SG). These main parts are linked by a mechanical drivetrain attached to the engine's crankshaft. The SG's electrical frequency f_e is related to the engine's speed ω_m by (1), where n_p is the SG's rotor pole pairs. As a result, the produced voltage frequency is directed by the DGS's engine rotational speed ($f_e = \omega_m \quad [\,\mathrm{pu}\,]$). The constant frequency operation (1pu) is achieved by the diesel engine's speed governor. From the powered load viewpoint, the SG converts the mechanical energy supplied by the diesel engine into electrical energy. The constant voltage (1pu) operation of the SG is insured by the so-called automatic voltage regulator (AVR).

$$2\pi f_e = n_p \omega_m \tag{1}$$

2.2 Diesel genset identification problem statement

The first part of the identification process is to write mathematical models according to DGS experimental data. Let us consider the structure of mechanical and electrical subsystems of the DGS depicted in Figs. 2 and 3 respectively. In the decoupled procedure proposed in the present paper, the estimation of DGS parameters defined in the vector θ (2) consists of separated estimation of parameters of the mechanical parameters sub vector θ_M (3) and electrical parameters sub vector θ_E (4).

$$\theta = \left[\theta_M \;\vdots\; \theta_E\right]^T \tag{2}$$

$$\theta_M = \left[T_a \quad T_c \quad T_d \quad D \quad H \quad K_P \quad K_I\right]^T \tag{3}$$

$$\theta_E = \left[x_d \quad x'_d \quad T'_{do} \quad T_A \quad T_B \quad T_C \quad T_R \quad K_A\right]^T \tag{4}$$

The identification procedure is explained by flowchart illustrated in Figure 4. The estimation algorithm proposed in this paper is well explained in [16] and resumed in Figure 4. Two selected tests are carried out for identification procedure implementation. The first, that is the rejection of a resistive load will allow the estimation of mechanical parameters while, the rejection of a purely capacitive load will yield electrical parameters identification. State space modelling enables an efficient analysis and simulation aforementioned parts.

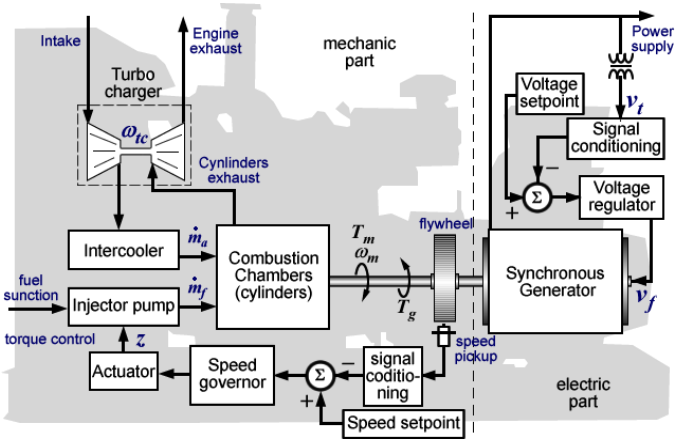

Figure 1. Diesel generator set block diagram.

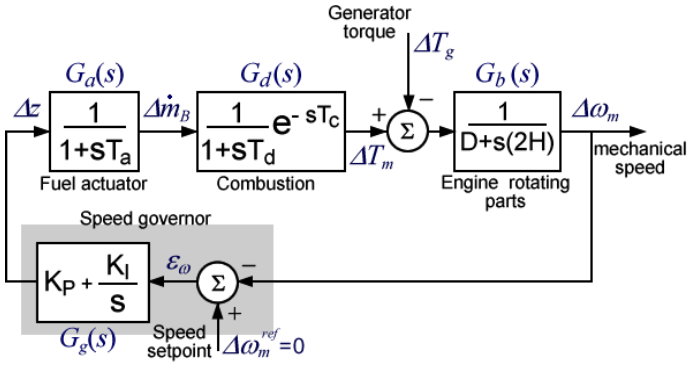

Figure 2. Diesel genset mechanical subsystem structure

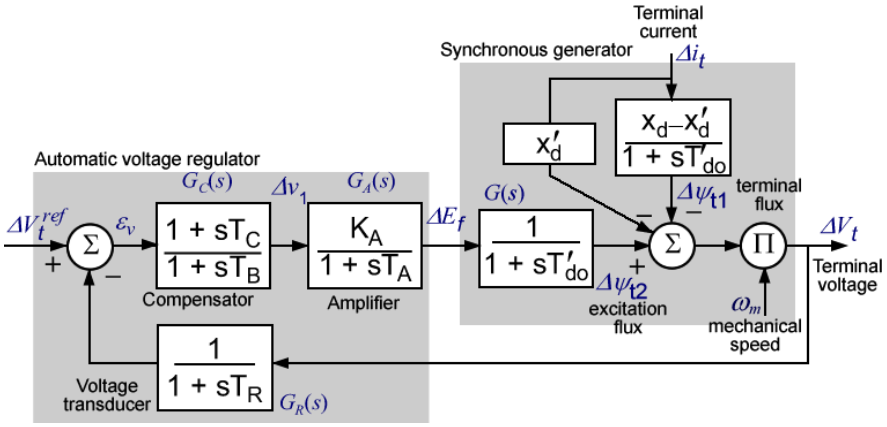

Figure 3 Diesel genset electric subsystem structure

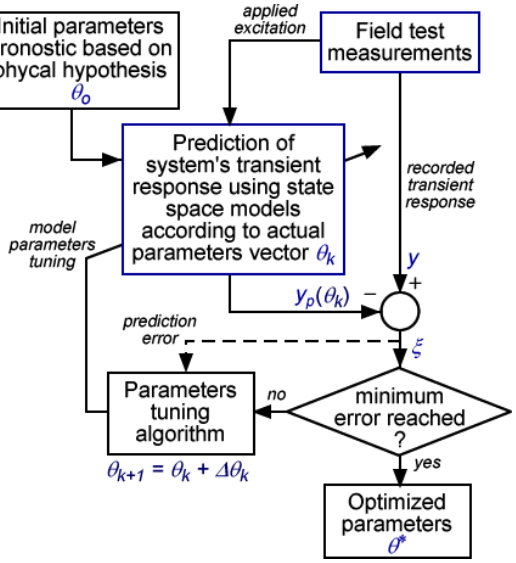

Figure 4. Flowchart for the parameters identification loop (based on [16])

3. DGS System modelling

This section deals with modelling of the DGS system. Block diagrams shown in Figs. 2 and 3 are reworded in terms of compact state space models to efficiently apply in the estimation process.

3.1 Diesel prime mover and speed governor

Figure 2 shows a simplified model that can adequately represent most of the dynamic behaviour of a diesel engine. The main phenomena taken into account are: a) the fuelling actuation, b) the combustion (torque production) and c) the engine's crankshaft torque balance. The fuelling actuator is modelled as a first-order transfer function $G_a(s)$ with unity gain (since the pu system is used) and time constant T_a. The engine's torque production is modelled by the time delay term e^{-sT_c} which represents the average time between a fuel flow $\Delta\dot{m}_B$ actuation and the subsequent power stroke. To derive a state model of the mechanical

part, a transient state model of the combustion bloc can be derived using a first-order Padé approximation of the combustion term as given by (4). This makes easier the derivation of the DGS state model given by (5), where Δx can be seen as an engine air supply related state variable, and $p()$ is the tine derivative operator. The Corresponding compact matrix form is given by (6) where mechanical part state and command matrices A_1 and B_1. This form allows a more thorough analysis of the closed-loop operation of the engine using linear algebra theory. It can be seen that state variables $\Delta\dot{m}_B$ and $\Delta\omega_m$ are physically measurable using suitable sensors. The synchronous generator's torque T_g is the mechanical part excitation input.

$$e^{-sT_c} \approx \frac{1-sT_c/2}{1+sT_c/2} = \frac{1-sT_c'}{1+sT_c'} \tag{4}$$

$$p\begin{bmatrix} \Delta x \\ \Delta T_m \\ \Delta\dot{m}_B \\ \Delta z \\ \Delta\omega_m \end{bmatrix} = \begin{bmatrix} -\frac{1}{T_d} & 0 & \frac{1}{T_d} & 0 & 0 \\ \frac{T_d+T_c'}{T_dT_c'} & -\frac{1}{T_c'} & -\frac{1}{T_d} & 0 & 0 \\ 0 & 0 & -\frac{1}{T_a} & \frac{1}{T_a} & 0 \\ 0 & -\frac{K_P}{2H} & 0 & 0 & \frac{DK_P}{2H}-K_I \\ 0 & \frac{1}{2H} & 0 & 0 & -\frac{D}{2H} \end{bmatrix} \begin{bmatrix} \Delta x \\ \Delta T_m \\ \Delta\dot{m}_B \\ \Delta z \\ \Delta\omega_m \end{bmatrix} + \begin{bmatrix} 0 \\ 0 \\ 0 \\ \frac{K_P}{2H} \\ -\frac{1}{2H} \end{bmatrix} \Delta T_g \tag{5}$$

$$\Rightarrow p(X_1) = A_1(\theta_M)X_1 + B_1(\theta_M)\Delta T_g \quad \text{and} \quad Y_1 = \Delta\omega_m \tag{6}$$

3.2 The synchronous generator

The Synchronous Generator (SG) converts the mechanical power produced by the diesel engine into electrical power. In this work, since the SG's rotor is usually integrated with the crankshaft of the diesel engine, the field connections are generally hard to access. This limits the number of possible standard tests ([13]) that can be done, thus one must carefully choose the parameters whose action is predominant in the transient behaviour of the DGS. The SG's terminal and rotor voltage equations are given by (7)-(9). In steady-state operation, the d-axis (resp. q-axis) voltage is created by the q-axis (resp. d-axis) flux.

As it can be seen throughout the standard std.421.5 [14], the transfer function giving the q-axis voltage v_q is solely considered when the generator is integrated in a voltage regulation loop. This is partly explained by the fact that the exciter, which is the main device that controls SG's rotor voltage v_f, also drives the d-axis flux ψ_d which is itself related to the q-axis voltage as shown by SG's terminal voltages equations (7)-(9). Thus, in this study, only the transient parameters related to the d-axis flux (hence the q-axis voltage) have been considered. This approximation is particularly suitable for medium and small-scale SGs for which sub-transients are not easy to catch using field testing. Furthermore, the highly noisy

environment of the DGS strongly affects measurements precision and the voltage regulation loop is designed to reject fast transients.

$$v_d = -r_a i_d - \omega_m \psi_q + \frac{1}{\omega_n} p(\psi_d) \quad (7)$$

$$v_q = -r_a i_q + \omega_m \psi_d + \frac{1}{\omega_n} p(\psi_q) \quad (8)$$

$$v_f = r_f i_f + \frac{1}{\omega_n} p(\psi_f) \quad (9)$$

A useful model for identifying SG parameters with dynamic field tests is obtained by defining its operational parameters ([11]-[13]). The main idea behind those parameters is the matchmaking of the main SG's terminal quantities. Transients of the d-axis stator flux $\Delta\psi_d$ is due to the combined action of the field voltage Δv_f and the d-axis current Δi_d as stated by (10)-(11) where $G(s)$ and $x_d(s)$ are the d-axis operational parameters. x'_d is the d-axis transient reactance and T'_{do} the transient time constant. The terminal voltage transient expression (14) is obtained by writing (10) in terms of transient variables and parameters. The influence of Δi_q is eliminated by considering just tests in which q-axis current is zero (e.g. purely reactive load rejections). The SG's bloc model is depicted in Figure 3 where $\Delta E_f = (x_{md}/r_f)\Delta v_f$. The identification test is chosen in order to ensure that $\omega_m \approx 1\text{pu}$; the SG's transient behavior is describes by equations (13)-(14) and output equation (15). These equations are connected to AVR model through ΔE_f and Δv_t.

$$\Delta\psi_d = G(s)\Delta v_f - x_d(s)\Delta i_d \quad (10)$$

$$x_d(s) = x'_d + \frac{x_d - x'_d}{1 + sT'_{do}} \quad \text{and} \quad G(s) = \frac{1}{1 + sT'_{do}} \frac{x_{md}}{r_f} \Delta v_f \quad (11)$$

$$\Delta V_t \approx \Delta v_q = r_a \Delta i_q + \omega_m \left(G(s)\Delta v_f - x_d(s)\Delta i_d \right) \quad (12)$$

$$p(\Delta\psi_{t1}) = -\frac{1}{T'_{do}} \Delta\psi_{t1} + \frac{x_d - x'_d}{T'_{do}} \Delta i_d \quad (13)$$

$$p(\Delta\psi_{t2}) = -\frac{1}{T'_{do}} \Delta\psi_{t2} + \frac{1}{T'_{do}} \Delta E_f \quad (14)$$

$$\Delta V_t = \Delta\psi_{t2} - \Delta\psi_{t1} - x'_d \Delta i_d \quad (15)$$

3.3 The voltage regulator

The automatic voltage regulator (AVR) modulates the SG's field voltage to maintain produced voltages at the fixed reference value (1pu). In a large majority of low and medium power diesel generators, this device is made of static power electronics rectifier and molded

into a plastic enclosure. The terminal voltage is compared to the reference (1pu) and the computed error is used to produce a correcting field voltage. From the standard std.421.5 [14] recommendations, the ST1A type static excitation system has been selected as the most suitable for our laboratory setup. A simplified diagram is shown in Figure 3. Special features like power stabilizer or field current/voltage limiters are ignored. So, we consider that system transient does not hit any limit during the analysis. The voltage transducer time constant T_R is also neglected by assuming a very fast voltage processing. The transient gain reduction (TGR) bloc allows the controlled rectifier dead time compensation and reinforces the closed-loop stability margins. The rectifier (amplifier) is modeled by a first-order transfer function with a static gain K_A and a time constant T_A. If the rectifier is fast enough, the use of TGR may not be critical for AVR stability. Based on Figure 3 diagram, equations governing the AVR transients are given by (16)-(18). By coupling AVR equations (17)-(19) to SG's equations (14)-(16), the state model given by (20) is derived. This form clearly shows that Δi_d is the main input affecting the electrical subsystem transients, especially for a reactive load (i.e. no current in q-axis)

$$p(\Delta v_2) = -\frac{1}{T_B}\Delta v_2 - \frac{T_B - T_C}{T_B^2}\Delta V_t \tag{16}$$

$$p(\Delta E_f) = \frac{K_A}{T_A}\Delta v_2 - \frac{1}{T_A}\Delta E_f - \frac{K_A T_C}{T_A T_B}\Delta V_t \tag{17}$$

$$\text{With} \quad \Delta v_1 = -\Delta v_2 - \frac{T_C}{T_B}\Delta V_t \quad \text{and} \quad \Delta E_f = \frac{x_{md}}{r_f}\Delta v_f \tag{18}$$

$$p\begin{bmatrix} \Delta v_2 \\ \Delta E_f \\ \Delta \psi_{t1} \\ \Delta \psi_{t2} \end{bmatrix} = \begin{bmatrix} \frac{-1}{T_B} & 0 & \frac{T_C - T_B}{T_B^2} & \frac{T_B - T_C}{T_B^2} \\ \frac{-K_A}{T_A} & \frac{-1}{T_A} & \frac{K_A T_C}{T_A T_B} & \frac{-K_A T_C}{T_A T_B} \\ 0 & 0 & \frac{-1}{T'_{do}} & 0 \\ 0 & \frac{1}{T'_{do}} & 0 & \frac{-1}{T'_{do}} \end{bmatrix} \begin{bmatrix} \Delta v_2 \\ \Delta E_f \\ \Delta \psi_{t1} \\ \Delta \psi_{t2} \end{bmatrix} + \begin{bmatrix} -\frac{T_B - T_C}{T_B^2} x'_d \\ \frac{K_A T_C}{T_A T_B} x'_d \\ \frac{x_d - x'_d}{T'_{do}} \\ 0 \end{bmatrix} \Delta i_d \tag{19}$$

$$\Rightarrow p(X_2) = A_2(\theta_E)X_2 + B_2(\theta_E)\Delta i_d \quad \text{and} \quad Y_2 = \Delta V_t \tag{20}$$

4. Tests modelling for identification process

This section will look at tests that may lead to parameter identification of a DGS according to the previously developed relationships.

4.1 Purely active load rejection test

When the DGS is loaded by a resistance bank, the supplied power, less the various losses, is directly supplied by the engine. The per-unit restive torque applied on the diesel engine

shaft is given by (21) where η_g is the SG's efficiency usually obtained from the rating plate. Since the engine speed is regulated, the mechanical speed $\omega_m \simeq \omega_m^{ref} = 1\,\text{pu}$.

$$T_{go} \approx \eta_g P_o / \omega_{mo} \tag{21}$$

If the active power is rejected by opening the DGS main breaker, the engine undergoes a negative torque step change. This excitation can be plugged in the previously developed diesel engine model. The engine speed $\Delta\omega_m$ transients are thereafter computed and used for θ_M parameter identification as shown in Figure 4. The engine operation mode is deduced by measuring steady-state speed before and after the load rejection. If there is no speed change, the governor is operating in isochronous mode. If there is a noticeable frequency variation, the steady state analysis shows that the speed governor gain is given by (22). Numeric value of D is normally very small compared to K_P. Remembering that combustion delay T_c' is related to the engine's torque update rate, its numerical value is approximated by (23) where N is the engine speed in rpm and n the number of cylinders.

$$\Delta\omega_{m\infty} = \frac{T_{go}}{K_P + D} \quad \Rightarrow \quad K_P \approx \frac{T_{go}}{\Delta\omega_{m\infty}} \tag{22}$$

$$T_c' \approx 30/nN \tag{23}$$

4.2 Purely reactive load rejection test

When a purely reactive load is connected to the DGS, the generator's electromagnetic torque is zero, and the mechanical part is not involved in the load rejection. The engine speed is therefore maintained to 1pu. Initial conditions prior to the reactive load rejection are given by (24) where ε is -1 for a capacitive load and +1 for an inductive load [13]. When the load is rejected, there is a step change in d-axis current. As for the mechanical part, the step change in d-axis current is synthesized and used in the identification loop depicted in Fig 4.

$$\begin{aligned} &\omega_{mo} = 1\text{pu};\ V_{to} = V_{qo} = 1\text{pu};\ V_{do} \approx 0; \\ &I_{qo} \approx 0;\quad I_{do} \approx \varepsilon I_{to};\quad I_{fo} \approx \frac{V_{to} + \varepsilon I_{to} x_{do}}{x_{md}} \end{aligned} \tag{24}$$

5. Identification results and discussions

In this section, we present identification results. The experimental setup and data measurements are shown in Fig. 5. Tests are performed on a laboratory DGS comprising constituted by: an $7.2\ \text{hp}$ engine and a $6.5\ \text{kVA}$ SG. System rated values are given in Table 1. Diesel engine's speed is sensed with a tachogenerator directly mounted at one end of the engine's shaft. All the 3-phase voltages are measured to facilitate the instantaneous voltage value extraction. The terminal current is also measured for initial condition assessments. Firstly, the purely resistive load rejection was performed in order to obtain the mechanical part parameters and secondly, reactive load rejection was performed for electrical part identification.

5.1 Estimation of Mechanical parameters

During the entire test, the breaker K1 stays open. DGS is started and a Y-connected resistive load of 4.1pu is connected across its terminals. The measured active power supplied by the unit is $P_o = 0.244\text{pu}$. Thus, the evaluated initial generator torque (34) is $T_{go} = 0.228\text{pu}$. The breaker K2 is opened, and the engine's speed is recorded with a digital oscilloscope. Figure 7 shows the obtained result. It can be seen that the analysed DGS has a natural frequency of about 0.85 Hz and the frequency transients have an overshot of 1.8 %. Identification process is achieved using the function "*fmincon( )*" of Matlab® optimization toolbox. Identified parameters are shown in Table 2. Conversions in SI units are used to check the plausibility of identified parameters.

5.2 Estimation of electrical parameters

During the closed-loop reactive load rejection test, the breaker K2 stays open. The DGS is started and a Y-connected capacitive load of 2.1pu is connected at his terminals. The measured reactive power of the DGS is $Q_o = 0.477\text{pu}$. The breaker K1 has been operated to reject the load, and the engine terminal voltages were recorded. Results are shown in Figure 8 and identified parameters are shown in Table 3. The last shows good accuracy of obtained results. Obtained parameters of the voltage regulator are consistent with the typical parameters given in the IEEE std.421 [14] and manufacturer's data.

Table 1 Diesel generator set rated and used base values

Diesel engine		**Generator base values**	
horsepower	7.2 hp	S_{base}	= 6500 VA
Rated speed	3600 rpm	I_{sbase}	= 25.5 A
construction	1 cylinder, flyweights based speed governor	V_{sbase}	= 169.7 V
Synchronous generator		Z_{sbase}	= 6.65 Ω
power	6.5 kVA / 5 kW	L_{sbase}	= 17.65 mH
voltage	3- phase 208 /120 V	ω_{base}	= 377 rad/sec.
Frequency	60 Hz	ω_{mbase}	= 377 rad/sec.
Efficiency	93.6 %	V_{fbase}	= 361.1 V
Voltage regulator		I_{fbase}	= 18 A
Static, half wave controlled rectifier based.		Z_{fbase}	= 20.1 Ω
		T_{base}	= 17.24 Nm

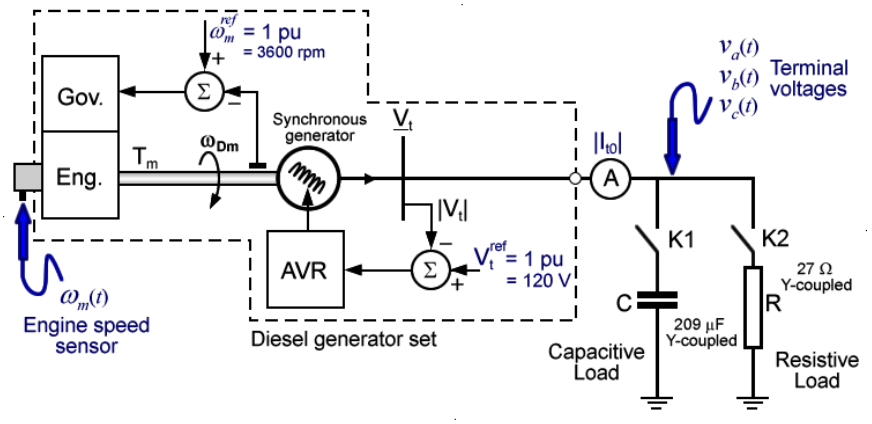

Figure 5. Experimental setup schematic diagram

Table 2 Estimated mechanical parameters in pu and SI

Parameters	Values	
Egine torque ipdate delay	T_c = 16.7 ms	-
Speed Governor gain	K_P = 16.863 pu	368.73 (SI)
Actuator time constant	T_a = 0.141 s	-
Air/fuel efficiency time constant	T_d = 0.141 s	-
Damping coefficient	D = 0.0003 pu	0.0068 Nms
Engine Rotor inertia	H = 1.1257 pu	0.103 Kgm^2

Table 3 Estimated electrical parameters

Part	Parameter	manufacturer	Proposed procedure
Synchronous generator	x_d [pu]	0.9330	0.857
	x'_d [pu]	0.0917	0.08
	T'_{do} [s]	0.2830	0.207
Voltage regulator	T_A [s]	-	0.0001
	T_B [s]	-	20.0
	T_C [s]	-	0.40
	K_A [pu]	-	200

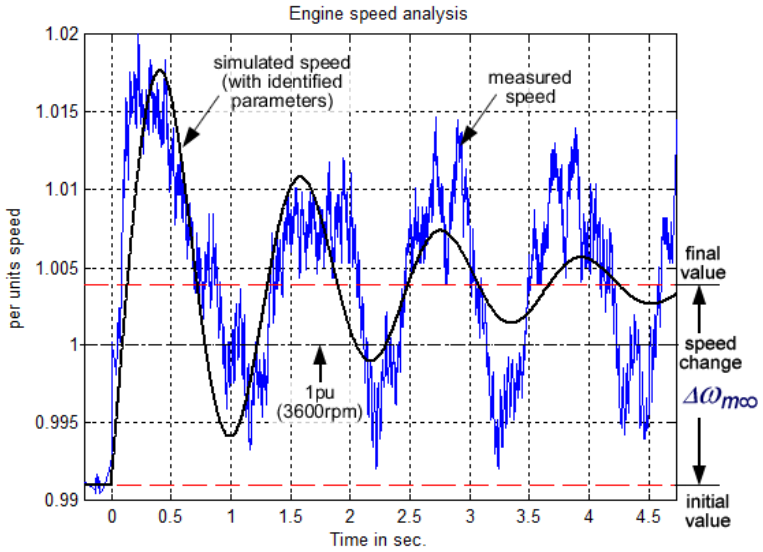

Figure 6. Speed transient following a purely resistive load rejection test

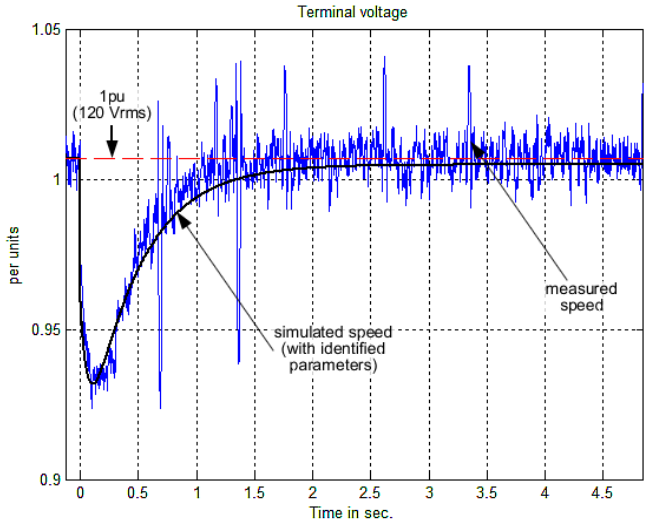

Figure 7. Terminal Voltage transient following a purely capacitive load rejection test

6. Conclusion

In this paper, the DGS system modelling has been addressed. Efficient modelling of the system has been carried out and then, the transient behaviours of DGS has been analysed. It has been shown that well-chosen load rejection tests can yield closed-loop system parameter identification. Accordingly, purely resistive and capacitive load rejection tests have been addressed for this purpose. Comparisons between estimated and experimental data have demonstrated the good accuracy of the estimation process. Future work is investigated to design appropriated test for parameter estimation of DGS, including q-axis SG's parameters.

7. References

[1] Roland Menges, "Supporting renewable energy on liberalized markets: green electricity between additionally and consumer sovereignty," *Energy Policy*, vol. 31, pp. 583–596, 2003

[2] Timothy M. Weis, Adrian Ilinca, Jean-Paul Pinard, "Stakeholders' perspectives on barriers to remote wind–diesel power plants in Canada," *Energy Policy*, vol. 36, pp. 1611–1621, 2008

[3] T. Senjyu, T. Nakaji, K. Uezato, and T. Funabashi, "A hybrid power system using alternative energy facilities in isolated island," *IEEE Transactions on Energy Conversion*, vol. 20, no. 2, pp. 406–414, June 2005

[4] T. Tameghe, R. Wamkeue and I. Kamwa, "Dynamic Model of Diesel Generator Set for Hybrid Wind-Diesel Small Grids Applications," *in CCECE, 25th IEEE Canadian Conference*, 2012

[5] I. Kamwa, "Dynamic modelling and robust regulation of a no-storage wind-diesel hybrid power system," *Electrical Power Systems Research*, vol. 18, pp. 219–233, 1990

[6] P. B. Malatestas, M. P. Papadopoulos and G. Starvrakakis, "Modeling and identification of diesel-wind turbines systems for wind penetration assessment, " *IEEE transaction on Power System*, Vol. 8, No 3, pp. 1091-1097, August 1993

[7] G. S. Stavrakakis and G. N. Kariniotakis, "A general simulation algorithm for the accurate assessment of isolated diesel- wind turbines systems interaction.," *IEEE Transactions on Energy Conversion,* vol. 10, no. 3, pp. 577–583, September 1995

[8] A.M. Sharaf and E.S. Abdin, "A digital simulation model for winddiesel conversion scheme," 26-28 Mar 1989, pp. 160–166

[9] Rakopoulos, Constantine D., Giakoumis, and Evangelos G., "Diesel Engine Transient Operation - Principles of Operation and Simulation Analysis," *Springer*, 2009

[10] G. Claeys, N. Retière, N. HdjSaid, P. Lmerle, E. Varret and R. Belhomme, "Dynamic modeling of turbo-charged diesel engine for power system studies," *22nd IEEE Power Engineering Society International Conference*, pp. 312-317, 2001

[11] I. Kamwa, R. Wamkeue, and X. Dai-Do, "General approaches to efficient d-q simulation and model translation for synchronous machines: a recap," *Electric Power Systems Research*, vol. 42, no. 3, pp. 173–180, September 1997

[12] R. Wamkeue, F. Baetscher, and I. Kamwa, “Hybrid state model based time-domain identification of synchronous machine parameters from saturated load rejection test records,” *IEEE Transactions on Energy Conversion*, vol. 23, no. 1, pp. 68–77, 2008

[13] IEEE Guide for Test Procedures for Synchronous Machines Part I Acceptance and Performance Testing Part II Test Procedures and Parameter Determination for Dynamic Analysis," *IEEE Std 115-2009 (Revision of IEEE Std 115-1995)*, pp.1-219, May 7 2010

[14] IEEE Recommended Practice for Excitation System Models for Power System Stability Studies," *IEEE Std 421.5-2005 (Revision of IEEE Std 421.5-1992)* , pp. 1-85, 2006

[15] Chow, J.H.; Glinkowski, M.T.; Murphy, R.J.; Cease, T.W.; Kosaka, N., "Generator and exciter parameter estimation of Fort Patrick Henry Hydro Unit 1," *IEEE Transactions on Energy Conversion,* vol.14, no.4, pp.923-929, Dec 1999

[16] Wamkeue, R.; Aguglia, D.; Lakehal, M.; Viarouge, P., "Two-Step Method for Identification of Nonlinear Model of Induction Machine," *IEEE Transactions on Energy Conversion,* vol.22, no.4, pp.801-809, Dec. 2007

9. Acknowledgements

This work was supported by the Industrial Innovation Scholarships (BMP Innovation) Program, offered jointly by CRSNG, FRQNT and IREQ.

10. Biography

Tommy A. Theubou Tameghe (S2010) received an MSc A. Degree from University of Quebec in Abitibi-Témiscamingue, Rouyn-Noranda, QC and is currently a Ph.D. student at the University of Quebec in Chicoutimi. The Thesis focuses on the analysis of integration techniques of distributed sources in actual power plants and smart grids.

René Wamkeue (S95, M98, and SM08) received the Ph.D. degree in electrical engineering from the École Polytechnique, Montreal, QC, Canada, in 1998. Since 1998, he has been with the Université du Québec en Abitibi-Témiscamingue, Rouyn-Noranda, QC, where he is currently a full professor of electrical engineering. His current research interests include control, power electronics, modelling, identification and diagnosis of electric machines, cogeneration and wind energy conversion systems. Prof. Wamkeue is a senior member of the IEEE/PES and acted as Secretary of the working group 7 for revision of IEEE Std-115.

Innocent Kamwa (IEEE Fellow, 2005) received the Ph.D. degree from Laval University, Québec City, QC, Canada, in 1988. He then joined Hydro-Québec's research institute (IREQ), where he is currently the chief scientist for Hydro-Québec's smart grid. He is a P. Eng. and Adjunct Professor of Power Systems Engineering at McGill University and Laval University. Dr. Kamwa serves on many IEEE/PES technical committees as member and officer, including the Fellow Evaluation, Electric Machinery, and Power System Stability committees.